Chirality Organization of Ferrocenes Bearing Podand Dipeptide Chains: Synthesis and Structural Characterization

Toshiyuki Moriuchi, Akihiro Nomoto, Kazuhiro Yoshida, Akiya Ogawa,† and Toshikazu Hirao*

Contribution from the Department of Applied Chemistry, Faculty of Engineering, Osaka University, Yamada-oka, Suita, Osaka 565-0871, Japan

Received August 2, 2000

Abstract: A variety of ferrocenes bearing podand dipeptide chains have been synthesized to form an ordered structure in both solid and solution states and have been investigated by ^{1}H NMR, FT-IR, CD, and X-ray crystallographic analyses. Conformational enantiomerization through chirality organization was achieved by the intramolecular hydrogen bondings between the podand dipeptide chains. The single-crystal X-ray structure determination of the ferrocene **2** bearing the podand dipeptide chains (-D-Ala-D-Pro-OEt) revealed two C_2-symmetric intramolecular hydrogen bondings between CO (Ala) and NH (another Ala) of each podand dipeptide chain to induce the chirality-organized structure. The molecular structures of the ferrocene **1** composed of the podand L-dipeptide chains (-L-Ala-L-Pro-OEt) and **2** are in a good mirror image relationship, indicating that they are conformational enantiomers. An opposite helically ordered molecular arrangement was formed in the crystal packing of **2** as compared with **1**. The ferrocene **2** exhibited induced circular dichroism (CD), which appeared at the absorbance of the ferrocene moiety. The mirror image of the CD signals between **1** and **2** was observed, suggesting that the chirality-organized structure via intramolecular hydrogen bondings is present even in solution. The ferrocene **4** bearing the podand dipeptide chains (-Gly-L-Leu-OEt) also showed an ordered structure in the crystal based on two intramolecular hydrogen bondings between CO (Gly) and NH (another Gly) of each podand dipeptide chain, together with intermolecular hydrogen bondings between CO adjacent to the ferrocene unit and NH (neighboring Leu) to create the highly organized self-assembly. A different self-assembly was observed in the crystal of the ferrocene **5** composed of the podand dipeptide chains (-Gly-L-Phe-OEt), wherein each molecule is bonded to two neighboring molecules through two pairs of symmetrical intermolecular hydrogen bonds to form a 14-membered intermolecularly hydrogen-bonded ring. These ordered structures based on the intramolecular hydrogen bondings in the solution state are also confirmed by ^{1}H NMR and FT-IR.

Introduction

Highly ordered molecular assemblies are constructed in protein to fulfill the unique functions as observed in enzymes, receptors, etc. Secondary structures such as α-helices, β-sheets, and β-turns play an important role in protein folding, which is mostly driven by hydrogen bonding and hydrophobic interaction of side chains.[1] Considerable effort has been focused on designing secondary structure mimetics composed of short peptides to gain insight into protein folding. In particular, the hydrogen-bonding capability of peptide strands to give chemical models of protein β-sheets has been investigated extensively by using template scaffolds such as a rigid aromatic,[2] an epindolidion,[3] a dibenzofuran,[4] an oligourea,[5] and an *endo-cis*-(2*S*,3*R*)-norbornene.[6]

Another important template is the ferrocenes, which are recognized as an organometallic scaffold for molecular receptors based on their redox properties and two rotatory coplanar cyclopentadienyl (Cp) rings with ca. 3.3 Å separation.[7] The inter-ring spacing of ferrocene is such that attached peptide

* To whom correspondence should be addressed.

† Present address: Department of Chemistry, Faculty of Science, Nara Women's University, Kitauoyanishi-machi, Nara 630-8506, Japan.

(1) (a) Schulz, G. E.; Schirmer, R. H. *Principles of Protein Structure*; Springer: New York, 1979. (b) Creighton, T. E. *Proteins: Structures and Molecular Properties*, 2nd ed.; Freeman: New York, 1993. (c) Kyte, J. *Structure in Protein Chemistry*; Garland: New York, 1995. (d) Branden, C.; Tooze, J. *Introduction to Protein Structure*, 2nd ed.; Garland: New York, 1998.

(2) (a) Feigel, M. *J. Am. Chem. Soc.* **1986**, *108*, 181. (b) Brandmeier, V.; Feigel, M.; Bremer, M. *Angew. Chem., Int. Ed. Engl.* **1989**, *28*, 486. (c) Brandmeier, V.; Feigel, M. *Tetrahedron* **1989**, *45*, 1365. (d) Brandmeier, V.; Sauer, W. H. B.; Feigel, M. *Helv. Chim. Acta* **1994**, *77*, 70.

(3) (a) Kemp, D. S.; Bowen, B. R. *Tetrahedron Lett.* **1988**, *29*, 5077. (b) Kemp, D. S.; Bowen, B. R. *Tetrahedron Lett.* **1988**, *29*, 5081. (c) Kemp, D. S. *Trends Biotechnol.* **1990**, *8*, 249. (d) Kemp, D. S.; Bowen, B. R.; Muendel, C. C. *J. Org. Chem.* **1990**, *55*, 4650.

(4) (a) Díaz, H.; Kelly, J. W. *Tetrahedron Lett.* **1991**, *32*, 5725. (b) Díaz, H.; Espina, J. R.; Kelly, J. W. *J. Am. Chem. Soc.* **1992**, *114*, 8316. (c) Díaz, H.; Tsang, K. Y.; Choo, D.; Espina, J. R.; Kelly, J. W. *J. Am. Chem. Soc.* **1993**, *115*, 3790. (d) Díaz, H.; Tsang, K. Y.; Choo, D.; Kelly, J. W. *Tetrahedron* **1993**, *49*, 3533. (e) Tsang, K. Y.; Díaz, H.; Graciani, N.; Kelly, J. W. *J. Am. Chem. Soc.* **1994**, *116*, 3988.

(5) (a) Nowick, J. S.; Powell, N. A.; Martinez, E. J.; Smith, E. M.; Noronha, G. *J. Org. Chem.* **1992**, *57*, 3763. (b) Nowick, J. S.; Abdi, M.; Bellamo, K. A.; Love, J. A.; Martinez, E. J.; Noronha, G.; Smith, E. M.; Ziller, J. W. *J. Am. Chem. Soc.* **1995**, *117*, 89. (c) Nowick, J. S.; Smith, E. M.; Noronha, G. *J. Org. Chem.* **1995**, *60*, 7386. (d) Nowick, J. S.; Mahrus, S.; Smith, E. M.; Ziller, J. W. *J. Am. Chem. Soc.* **1996**, *118*, 1066. (e) Nowick, J. S.; Holmes, D. L.; Mackin, G.; Noronha, G.; Shaka, A. J.; Smith, E. M. *J. Am. Chem. Soc.* **1996**, *118*, 2764. (f) Nowick, J. S.; Smith, E. M.; Pairish, M. *Chem. Soc. Rev.* **1996**, *25*, 401. (g) Nowick, J. S.; Pairish, M.; Lee, I. Q.; Holmes, D. L.; Ziller, J. W. *J. Am. Chem. Soc.* **1997**, *119*, 5413. (h) Nowick, J. S. *Acc. Chem. Res.* **1999**, *32*, 287.

(6) (a) Jones, I. G.; Jones, W.; North, M. *J. Org. Chem.* **1998**, *63*, 1505. (b) Ranganathan, D.; Haridas, V.; Kurur, S.; Thomas, A.; Madhusudanan, K. P.; Nagaraj, R.; Kunwar, A. C.; Sarma, A. V. S.; Karle, I. L. *J. Am. Chem. Soc.* **1998**, *120*, 8448.

10.1021/ja002869n CCC: $20.00
Published on Web 12/14/2000

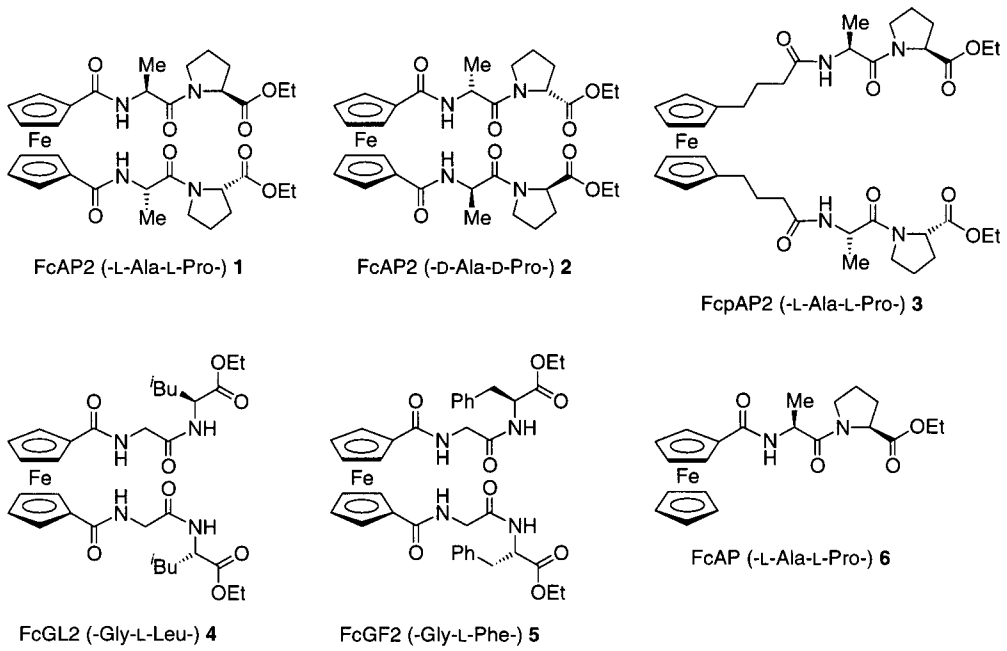

Figure 1. Ferrocenes bearing dipeptide chains.

strands are at a distance appropriate for hydrogen bonding. The utilization of ferrocene as a scaffold is considered to be one strategy to examine the hydrogen-bonding ability of peptide strands.[8] From this point of view, we recently embarked upon the introduction of the podand dipeptide chains (-L-Ala-L-Pro-OR) into ferrocene, providing an ordered structure based on two rigid intramolecular hydrogen bonds and a helical molecular arrangement in the crystal packing.[9] The advantage in the use of L-alanyl-L-proline as a dipeptide depends on there being a hydrogen-bonding site and a sterically constrained proline as a well-known turn inducer in proteins.

On the other hand, conformational enantiomers based on the torsional twist about the Cp(centroid)−Fe−Cp(centroid) axis are possible in the case of the 1,1′-disubstituted ferrocene as shown in Figure 4.[10] Generally, conformational enantiomers interconvert with ease due to the low barrier of Cp ring twisting. The introduction of peptide chains into ferrocene is envisaged to induce conformational enantiomerization by restriction of the torsional twist through chirality organization based on the intramolecular hydrogen bondings. In this context, we herein describe the synthesis and structural characterization of a variety of ferrocenes bearing podand dipeptide chains to elucidate the chirality and self-assembling organization.

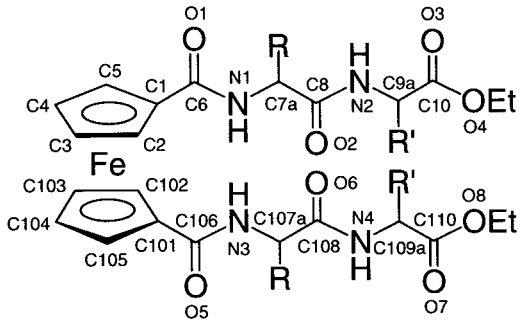

Figure 2. Numbering of selected atoms of ferrocenes bearing dipeptide chains.

Results and Discussion

The ferrocenes bearing podand dipeptide chains were synthesized from the corresponding 1,1′-bis(chlorocarbonyl)ferrocene and dipeptide ethyl ester hydrogen chloride. The thus-obtained ferrocenes were fully characterized by spectral data and elemental analyses. Ferrocenes bearing podand dipeptide chains exhibited an appropriate reversible redox wave attributable to the Fe(II)/Fe(III) couple (Table 1).

X-ray crystallographic analyses were performed in order to clarify ordered structures and self-assembling properties of ferrocenes bearing podand dipeptide chains (Tables 2−5). The incorporation of the podand dipeptide chains (-L-Ala-L-Pro-OEt) into ferrocene has been demonstrated to achieve an ordered structure based on two rigid intramolecular hydrogen bondings, and the novel helically ordered arrangement is realized in the crystal packing of **1**.[9] To evaluate the ability of ferrocenes bearing podand dipeptide chains to induce conformational enantiomerization, the crystal structure of **2** bearing the corresponding podand D-dipeptide chains (-D-Ala-D-Pro-OEt) was investigated. The crystal structure of **2** revealed the formation of two C_2-symmetric intramolecular hydrogen bondings between CO (Ala) and NH (another Ala) of each podand dipeptide chain (N(1)···O(2*), 2.981 Å) (Figure 3b and Table 4). Although a wide range of relative orientations is possible depending on two rotatory Cp rings, the podand dipeptide chains are arrayed in the same direction, based on two intramolecular hydrogen bonds

(7) (a) Saji, T.; Kinoshita, I. *J. Chem. Soc., Chem. Commun.* **1986**, 716. (b) Medina, J. C.; Li, C.; Bott, S. G.; Atwood, J. L.; Gokel, G. W. *J. Am. Chem. Soc.* **1991**, *113*, 366. (c) Medina, J. C.; Goodnow, T. T.; Rojas, M. T.; Atwood, J. L.; Lynn, B. C.; Kaifer, A. E.; Gokel, G. W. *J. Am. Chem. Soc.* **1992**, *114*, 10583. (d) Beer, P. D. *J. Chem. Soc., Chem. Commun.* **1996**, 689. (e) Beer, P. D.; Graydon, A. R.; Johnson, A. O. M.; Smith, D. K. *Inorg. Chem.* **1997**, *36*, 2112. (f) Li, C.; Medina, J. C.; Maguire, G. E. M.; Abel, E.; Atwood, J. L.; Gokel, G. W. *J. Am. Chem. Soc.* **1997**, *119*, 1609.

(8) (a) Eckert, H.; Seidel, C. *Angew. Chem., Int. Ed. Engl.* **1986**, *25*, 159. (b) Herrick, R. S.; Jarret, R. M.; Curran, T. P.; Dragoli, D. R.; Flaherty, M. B.; Lindyberg, S. E.; Slate, R. A.; Thornton, L. C. *Tetrahedron Lett.* **1996**, *37*, 5289. (c) Kira, M.; Matsubara, T.; Shinohara, H.; Sisido, M. *Chem. Lett.* **1997**, 89. (d) Kraatz, H.-B.; Lusztyk, J.; Enright, G. D. *Inorg. Chem.* **1997**, *36*, 2400. (e) Okamura, T.; Sakauye, K.; Ueyama, N.; Nakamura, A. *Inorg. Chem.* **1998**, *37*, 6731.

(9) (a) Nomoto, A.; Moriuchi, T.; Yamazaki, S.; Ogawa, A.; Hirao, T. *Chem. Commun.* **1998**, 1963. (b) Moriuchi, T.; Nomoto, A.; Yoshida, K.; Hirao, T. *J. Organomet. Chem.* **1999**, *589*, 50.

(10) (a) Cerichelli, G.; Floris, B.; Ortaggi, G. *J. Organomet. Chem.* **1974**, *76*, 73. (b) Togni, A.; Hayashi, T. *Ferrocenes*; VCH: Weinheim, 1995.

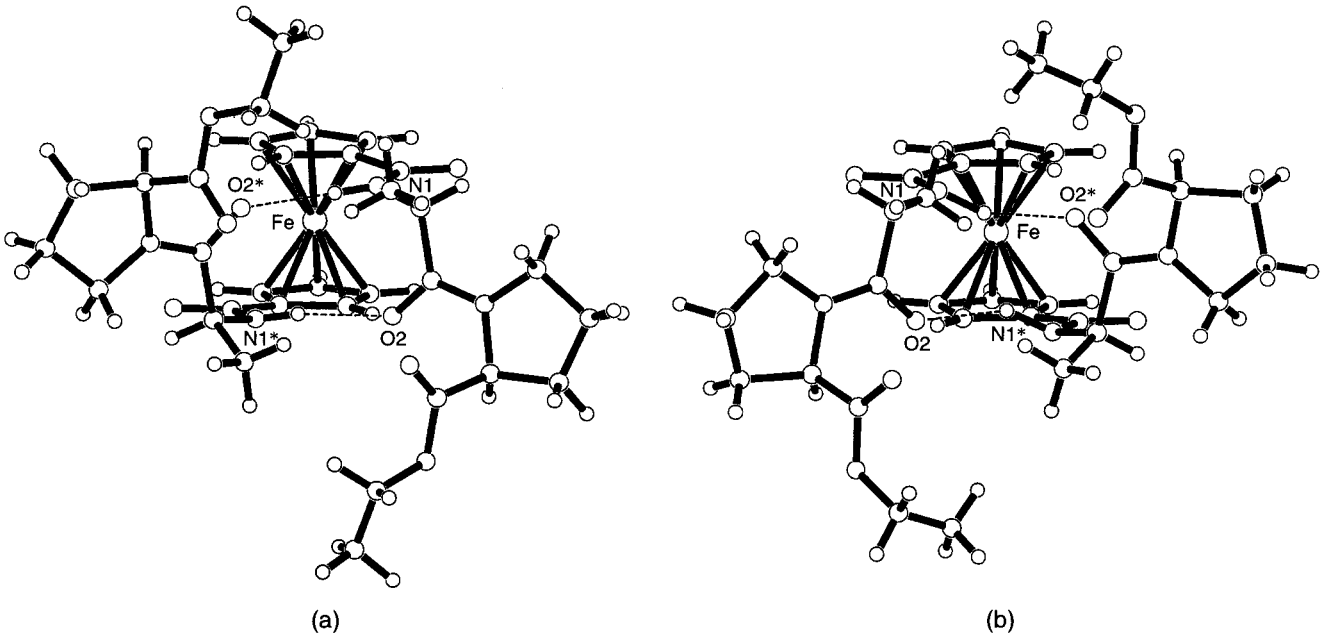

Figure 3. Molecular structures of (a) **1** and (b) **2**.

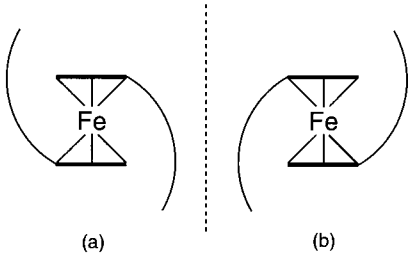

Figure 4. Enantiomorphous conformations. The enantiomorphs are related by the mirror plane. Schematic representations of (a) **1** and (b) **2**.

Table 1. Selected Spectroscopic Data for **1**−**6**

	^{1}H NMR N−H (ppm)[a]		FT-IR ν_{N-H} (cm^{-1}),[a]	$E_{1/2}$ (V),[b]
	$CDCl_3$	$CDCl_3$/DMSO-d_6 (9:1)	CH_2Cl_2	Fc/Fc$^+$, CH_2Cl_2
1[c]	8.96	8.95	3302	0.31
2	8.96	8.95	3302	0.31
3	6.70	7.04	3413	−0.12
			3321	
4	8.58	8.73	3417	0.35
	6.46	7.71	3317	
5	8.59	8.64	3410	0.33
	6.47	7.68	3321	
6[c]	6.66[d]	6.85[d]	3415[d]	0.17

[a] 1.0×10^{-2} M. [b] Volts vs Fc/Fc$^+$ as an internal standard. [c] Reference 9. [d] 2.0×10^{-2} M.

to induce an ordered structure. The molecular structures of **1** composed of the podand dipeptide chains (-L-Ala-L-Pro-OEt) and **2** are in a good mirror image relationship, as shown in Figure 3, indicating that they are conformational enantiomers (Figure 4). The opposite values of the torsion angles of **2** as compared with those of **1** also support the enantiomorphous conformations (Table 5). These results indicate that the introduction of the chiral dipeptide chains into ferrocene induces the chiral molecular arrangement based on an ordered structure via intramolecular hydrogen bondings.

The crystals of **1** bearing L-isomer and **2** bearing D-isomer belong to the same space group, $I4_1$. The ferrocene **2** was found to be packed in a novel helically ordered arrangement with one

Table 2. Crystallographic Data for **2**, **4**, and **5**

	2	**4**[a]	**5**
formula	$C_{32}H_{42}N_4O_8Fe$	$C_{32}H_{46}N_4O_8Fe$	$C_{38}H_{42}N_4O_8Fe$
fw	666.55	670.58	738.62
cryst syst	tetragonal	triclinic	orthorhombic
space group	$I4_1$ (No. 80)	$P1$ (No. 1)	$C222_1$ (No. 20)
a, Å	14.573(2)	9.294(1)	10.8188(7)
b, Å		11.783(1)	21.434(1)
c, Å	14.953(2)	8.924(1)	16.306(1)
α, deg		98.65(1)	
β, deg		116.481(9)	
γ, deg		81.41(1)	
V, Å^3	3175.7(8)	861.0(2)	3781.2(4)
Z	4	1	4
D_{calcd}, g cm^{-3}	1.394	1.293	1.297
μ(Mo Kα), cm^{-1}	5.31	4.90	4.53
T, °C	23	23	23
λ(Mo Kα), Å	0.71069	0.71069	0.71069
R[b]	0.052	0.039	0.056
R_w[c]	0.037	0.030	0.059

[a] Further refined data. [b] $R = \sum||F_o| - |F_c||/\sum|F_o|$. [b] $R_w = [\sum w(|F_o| - |F_c|)^2/\sum w|F_o|^2]1^{1/2}$.

turn of 14.95 Å pitch height, within which the distance between the closest ferrocene units is 4.46 Å. It is in sharp contrast to the finding that **1** forms an opposite helically ordered arrangement (Figure 5a,b). Furthermore, the ferrocene moieties arrange in a herringbone motif, and the proline and ethyl ester moieties individually form the columns (Figure 5c,d). These molecular arrangements show a good mirror image relationship. The podand dipeptide chains (−Ala-Pro-OEt) are considered to induce such molecular aggregation through interaction of a hydrogen-bonding site (Ala) and a hydrophobic moiety (Pro).

In the ^{1}H NMR spectra of **2** in $CDCl_3$ (1.0×10^{-2} M), only one kind of N−H resonance was detected at a lower field (8.96 ppm) than that of the ferrocene **6** bearing only one dipeptide chain (-L-Ala-L-Pro-OEt) (2.0×10^{-2} M, 6.66 ppm).[9] The N−H resonance of **2** was not perturbed by the addition of aliquots of DMSO-d_6 to $CDCl_3$, although a slightly downfield shift was observed with **6** (Table 1). These results indicate that two identical intramolecular hydrogen bonds between the podand dipeptide chains of **2** appear to be present even in solution. The FT-IR spectrum of **2** in CH_2Cl_2 (1.0×10^{-2} M) showed only

Table 3. Selected Bond Distances (Å) and Angles (deg) for **2**, **4**, and **5**

	2[a]	**4**	**5**[a]
	Bond Distances		
Fe−C(1)	2.02(1)	2.034(4)	2.03(1)
Fe−C(2)	2.07(1)	2.043(4)	2.01(1)
Fe−C(3)	2.06(1)	2.049(4)	2.02(1)
Fe−C(4)	2.10(1)	2.036(4)	2.02(2)
Fe−C(5)	2.03(1)	2.024(4)	1.98(1)
Fe−C(101)		2.027(3)	
Fe−C(102)		2.029(4)	
Fe−C(103)		2.047(4)	
Fe−C(104)		2.038(4)	
Fe−C(105)		2.037(4)	
C(1)−C(6)	1.51(1)	1.476(4)	1.44(1)
C(101)−C(106)		1.476(4)	
C(6)−O(1)	1.225(10)	1.227(3)	1.25(1)
C(106)−O(5)		1.237(3)	
C(6)−N(1)	1.33(1)	1.345(4)	1.36(1)
C(106)−N(3)		1.329(4)	
N(1)−C(7a)	1.458(10)	1.440(4)	1.45(2)
N(3)−C(107a)		1.435(4)	
C(8)−O(2)	1.221(9)	1.239(4)	1.21(1)
C(108)−O(6)		1.222(4)	
	Bond Angles		
C(2)−C(1)−C(6)	127.5(9)	128.7(3)	128(1)
C(102)−C(101)−C(106)		127.5(3)	
C(5)−C(1)−C(6)	124(1)	123.8(3)	127(1)
C(105)−C(101)−C(106)		125.0(3)	
C(1)−C(6)−N(1)	115.5(9)	117.1(3)	118.5(9)
C(101)−C(106)−N(3)		117.4(3)	
O(1)−C(6)−N(1)	124.5(9)	122.2(3)	119(1)
O(5)−C(106)−N(3)		121.2(3)	
C(6)−N(1)−C(7a)	118.1(8)	120.4(3)	121.8(10)
C(106)−N(3)−C(107a)		120.7(3)	

[a] The molecule sits on an inversion center.

Table 4. Hydrogen Bonds for **2**, **4**, and **5**

crystal	type[a]	donor	acceptor	D···A (Å)	D−H···A (deg)
2[b]	intra	N(1)	O(2*)	2.981(8)	146(5)
	intra	N(1*)	O(2)	2.981(8)	146(5)
4	intra	N(1)	O(6)	3.042(3)	163(3)
	intra	N(3)	O(2)	2.753(4)	155(2)
	inter	N(2)	O(5a)	2.765(3)	149(2)
	inter	N(4)	O(1b)	2.988(3)	168(3)
	inter	N(4c)	O(1)	2.988(3)	168(3)
	inter	N(2d)	O(5)	2.765(3)	149(2)
5[b]	intra	N(1)	O(2*)	2.84(1)	163(8)
	intra	N(1*)	O(2)	2.84(1)	163(8)
	inter	N(2)	O(1a)	2.87(1)	161(7)
	inter	N(2a)	O(1)	2.87(1)	161(7)
	inter	N(2*)	O(1b)	2.87(1)	161(7)
	inter	N(2b)	O(1*)	2.87(1)	161(7)

[a] Inter, intermolecular; intra, intramolecular. [b] The molecule sits on an inversion center.

one N−H stretching band at 3302 cm^{-1}, which also supports the hydrogen bonding in **2**. To gain insight into the effect of spacer on intramolecular hydrogen bonding, the ferrocene **3** bearing the podand dipeptide chains (-$CH_2CH_2CH_2$CO-L-Ala-L-Pro-OEt) was prepared. The amide N−H signal at 6.70 ppm in ^{1}H NMR and the amide N−H stretching band at 3413 cm^{-1} in FT-IR suggest that such an intramolecular hydrogen bond as observed in **1** and **2** is not likely to be formed in the case of **3**, possibly due to the rotation of the Cp rings of the ferrocene moiety. The presence of a small, broad band at 3321 cm^{-1} in the FT-IR spectrum of **3** indicates that there is a small fraction of a hydrogen-bonded conformation. Circular dichroism (CD) spectrometry is a useful tool to determine an ordered structure in solution. The ferrocene **2** exhibited an induced CD around the absorbance of the ferrocene function, although such an induced CD was not detected in the case of **3** (Figure 6). The mirror image of the CD signals observed with the L-isomer was obtained in the CD spectrum of **2**, indicating that a chiral molecular arrangement based on an ordered structure via intramolecular hydrogen bondings is formed even in solution.

Among the factors that induce the self-assembly processes, design of the ligand plays an important role. The dipeptide chain (-Gly-L-Leu-OEt) is expected to show different propensities of molecular arrangement based on two hydrogen-bonding sites. The X-ray crystal structure of the ferrocene **4** bearing the podand dipeptide chains (-Gly-L-Leu-OEt) was also characterized by two intramolecular hydrogen bondings between CO (Gly) and NH (another Gly) of each podand dipeptide chain (N(1)···O(6), 3.042 Å; N(3)···O(2), 2.753 Å) to induce the chirality-organized structure, which adopts the same conformation as that observed in **1** (Figure 7). The NH of the Leu in this conformation is available for participating in intermolecular hydrogen bonding with CO adjacent to the ferrocene unit, as shown in Figure 8, creating the highly organized self-assembly in the crystal packing, wherein each molecule is connected to four neighboring molecules through NH···O═C bonds (N(2)···O(5a), 2.765 Å; N(4)···O(1b), 2.988 Å; N(2d)···O(5), 2.765 Å; N(4c)···O(1), 2.988 Å).

Protein folding is driven by not only the hydrogen bonding but also the hydrophobic effect.[11] The kind and grouping of amino acid side chains are known to determine protein secondary structures. To evaluate the effect of side chains in the self-assembly, the ferrocene **5** bearing the podand dipeptide chains (-Gly-L-Phe-OEt) was examined. The X-ray crystal structure of the ferrocene **5** showed the same ordered structure based on two C_2-symmetric intramolecular hydrogen bondings between CO (Gly) and NH (another Gly) of each podand dipeptide chain (N(1)···O(2*), 2.84 Å) (Figure 9). However, the ferrocene **5** exhibited a different self-assembly in the crystal (Figure 10). Each molecule is bonded to two neighboring molecules, wherein each podand dipeptide chain forms a 14-membered intermolecularly hydrogen-bonded ring with the podand dipeptide chain of the neighboring molecule through two pairs of symmetrical intermolecular hydrogen bonds (N(2)···O(1a), 2.87 Å; N(2a)···O(1), 2.87 Å).

Table 5. Torsion Angles (deg) for **1**, **2**, **4**, and **5**

	angle[a]	**1**[b,c]	**2**[b]	**4**	**5**[b]
ϕ_1	C(6)−N(1)−C(7a)−C(8)	−86.0(6)	81.3(9)	−93.4(3)	−66(1)
ψ_1	N(1)−C(7a)−C(8)−N(2)	159.9(5)	−159.2(7)	151.9(3)	163.5(9)
ω_1	C(7a)−C(8)−N(2)−C(9a)	167.4(5)	−172.1(8)	174.3(3)	178(1)
ϕ_2	C(8)−N(2)−C(9a)−C(10)	−64.9(7)	71(1)	−162.1(3)	−57(1)
ψ_2	N(2)−C(9a)−C(10)−O(4)	157.0(5)	−167.5(8)	108.5(3)	138.3(8)
ϕ_1*	C(106)−N(3)−C(107a)−C(108)			−72.1(4)	
ψ_1*	N(3)−C(107a)−C(108)−N(4)			146.9(3)	
ω_1*	C(107a)−C(108)−N(4)−C(109a)			−176.7(3)	
ϕ_2*	C(108)−N(4)−C(109a)-C(110)			−115.9(3)	
ψ_2*	N(4)−C(109a)−C(110)−O(8)			161.0(3)	

[a] Symbol used for torsion angles in peptides (IUPAC−IUB Commission on Biochemical Nomenclature). [b] The molecule sits on an inversion center. [c] Reference 9.

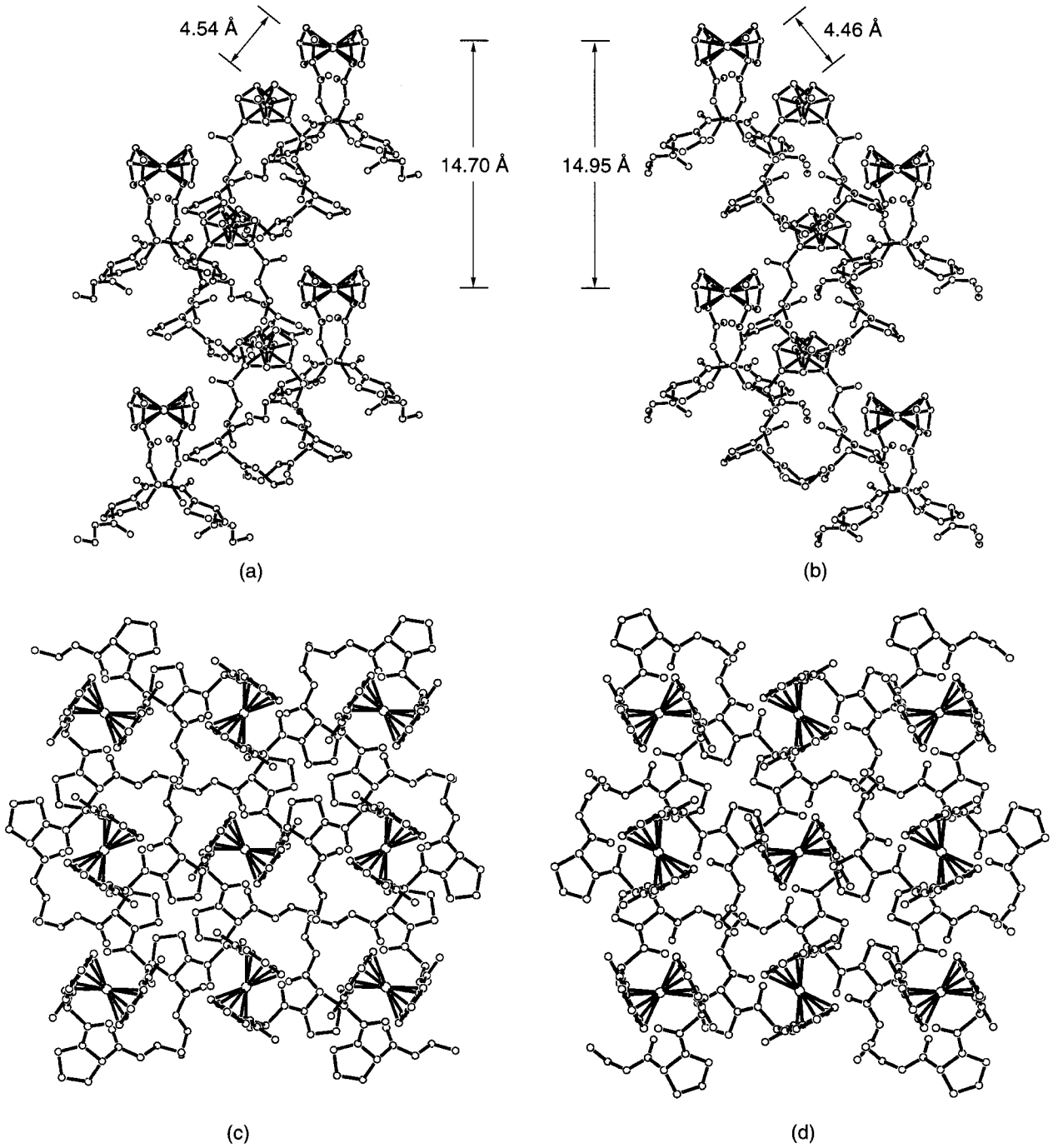

Figure 5. Top view of a portion of a layer containing the helical arrangement of crystal packing of (a) **1** and (b) **2**, and side view of crystal packing of (c) **1** and (d) **2**.

The ferrocene **4** bearing the podand dipeptide chains (-Gly-L-Leu-OEt) and the ferrocene **5** bearing the podand dipeptide chains (-Gly-L-Phe-OEt) exhibited hydrogen-bonded (**4**, 3317 cm^{-1}; **5**, 3321 cm^{-1}) and non-hydrogen-bonded N−H stretching bands (**4**, 3417 cm^{-1}; **5**, 3410 cm^{-1}) in FT-IR. The hydrogen-bonded (**4**, 8.58 ppm; **5**, 8.59 ppm) and non-hydrogen-bonded (**4**, 6.46 ppm; **5**, 6.47 ppm) N−H resonances were also observed in ^{1}H NMR. From these findings, the ferrocenes **4** and **5** are likely to form an ordered structure via intramolecular hydrogen bonding, as observed in the crystal structure, although the N−H of -L-Leu- and -L-Phe-, respectively, is not supposed to participate in the hydrogen bonding in solution.

(11) (a) Kauzmann, W. *Adv. Protein Chem.* **1959**, *14*, 1. (b) Tanford, C. *The Hydrophobic Effect*; Wiley and Sons: New York, 1973. (c) Blake, C. C. F.; Geisow, M. J.; Oatley, S. J.; Rérat, B.; Rérat, C. *J. Mol. Biol.* **1978**, *121*, 339. (d) Rose, G. D.; Roy, S. *Proc. Natl. Acad. Sci. U.S.A.* **1980**, *77*, 4643. (e) Dill, K. A. *Biochemistry* **1990**, *29*, 7133.

Conclusion

Structural and self-assembling characterization of a variety of ferrocenes bearing podand dipeptide chains in both solid and solution states was investigated by ^{1}H NMR, FT-IR, CD, and X-ray crystallographic studies. The ferrocene was found to serve as a reliable organometallic scaffold for the construction of an ordered structure via intramolecular hydrogen bondings. Conformational enantiomerization through chirality organization was achieved by restriction of the torsional twist based on the intramolecular hydrogen bond between podand peptide chains. An intrinsic induced CD around the absorbance of the ferrocene

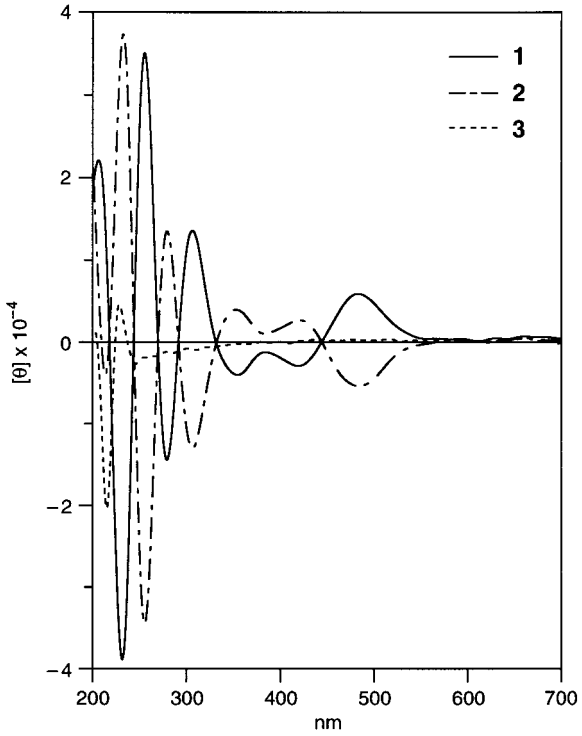

Figure 6. CD spectra of **1**, **2**, and **3** in MeCN (1.0×10^{-4} M).

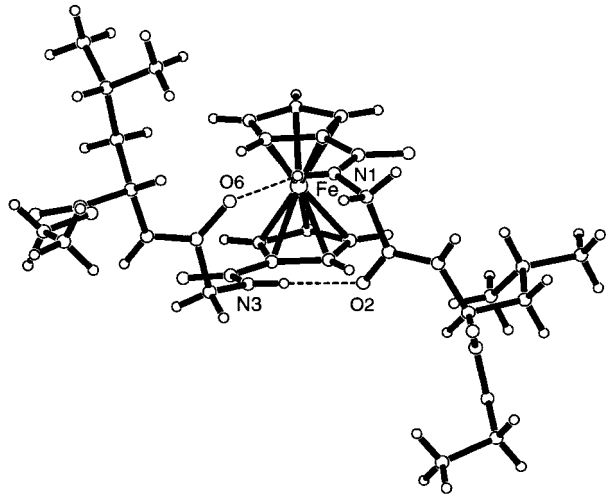

Figure 7. Molecular structure of **4**.

function indicates the presence of the chirality-organized structure via intramolecular hydrogen bondings even in solution. A striking feature is that a good mirror image relationship of the molecular structure of **1** and **2** based on conformational enantiomerization is realized. Furthermore, a mutually opposite helically ordered molecular arrangement was observed in their crystal packings, which is probably induced by a hydrogen-bonding site (Ala) and a sterically constrained moiety (Pro).

Another noteworthy feature of the ferrocenes bearing podand dipeptide chains is their strong tendency to self-assemble through contribution of all available hydrogen-bonding donors in the solid state. The NH of the Leu in the ferrocene **4** is available to participate in intermolecular hydrogen bonding with CO adjacent to the ferrocene unit, creating the highly organized self-assembly in the crystal packing, wherein each molecule is connected to four neighboring molecules. In the case of the ferrocene **5**, each molecule is bonded to two neighboring molecules, wherein each podand dipeptide chain forms a 14-membered intermolecularly hydrogen-bonded ring through two pairs of symmetrical inter-

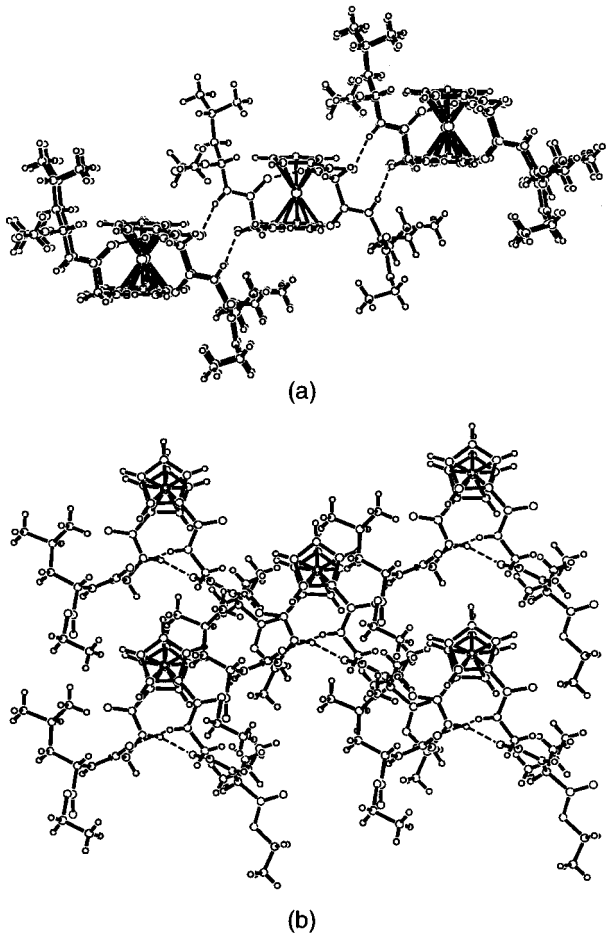

Figure 8. (a) Top view and (b) side view of a hydrogen-bonded chain assembly of **4**.

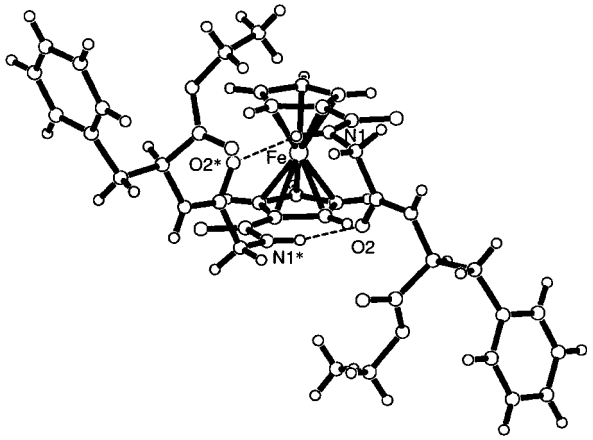

Figure 9. Molecular structure of **5**.

molecular hydrogen bonds between the NH of the Phe and CO adjacent to the ferrocene unit. The architectural control of molecular assemblies by use of peptide chains possessing chiral centers and hydrogen-bonding sites is considered to be a useful approach to artificial highly ordered supramolecular systems.

Studies on the application of chirality organization of ferrocenes bearing podand dipeptide chains for molecular recognition are in progress.

Experimental Section

General Methods. All reagents and solvents were purchased from commercial sources and were further purified by the standard methods, if necessary. Melting points were determined on a Yanagimoto

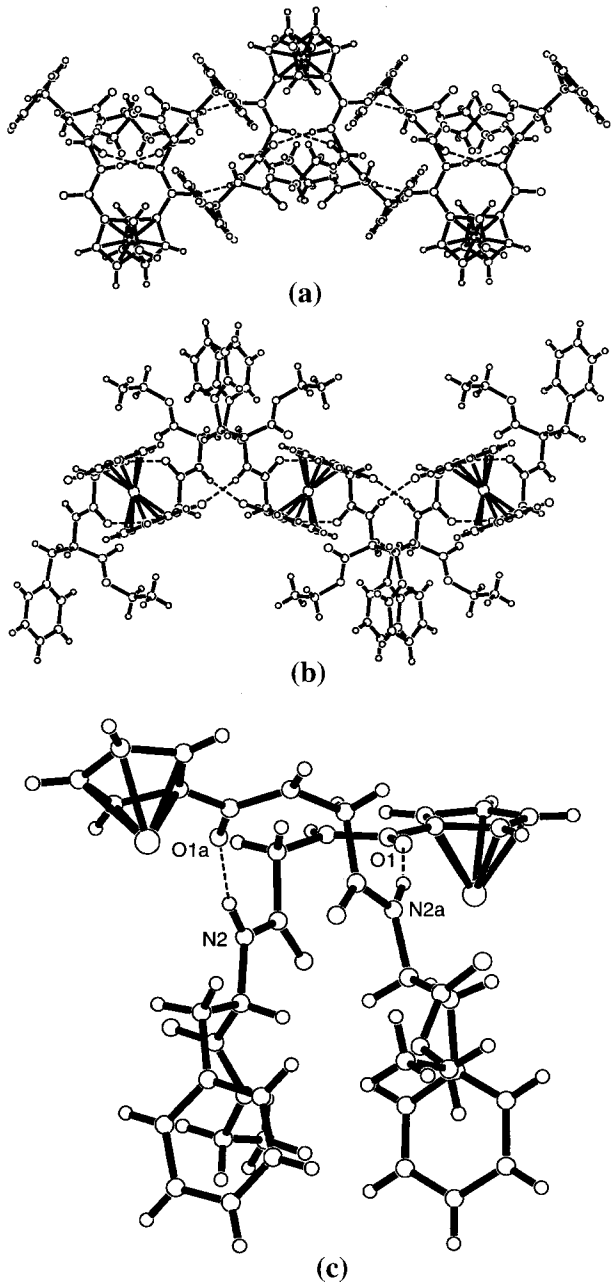

Figure 10. (a) Top view and (b) side view of a self-assembly of **5** via the formation of a 14-membered intermolecularly hydrogen-bonded ring. (c) A 14-membered intermolecularly hydrogen-bonded ring of **5**. Only half of the molecule is shown for clarity.

micromelting point apparatus and were uncorrected. Infrared spectra were obtained with a Perkin-Elmer model 1605 FT-IR. ^{1}H NMR spectra were recorded on JEOL JNM-GSX-400 (400 MHz) and JEOL JNM-ECP 400 (400 MHz) spectrometers with tetramethylsilane as an internal standard. Mass spectra were run on a JEOL JMS-DX303HF mass spectrometer. Peptide ester hydrogen chlorides were prepared by esterification of the commercially available dipeptide with an alcohol under acidic conditions.

General Procedure for the Synthesis of Ferrocenes Bearing the Podand Dipeptide Chains. To a stirred mixture of the dipeptide ethyl ester hydrogen chloride (0.60 mmol) and triethylamine (418 μL, 3.0 mmol) in dichloromethane (4 mL) was added 1,1′-bis(chlorocarbonyl)-ferrocene (93.3 mg, 0.30 mmol) in dichloromethane (6 mL) dropwise under argon at 0 °C. The mixture was stirred at 0 °C for 1 h and then at room temperature for 1 h. The resulting mixture was diluted with dichloromethane, washed with saturated $NaHCO_3$ aqueous solution and brine, and then dried over Na_2SO_4. The solvent was evaporated in vacuo, and the residue was chromatographed on an alumina column, eluting with dichloromethane. The ferrocene was isolated by recrystallization from dichloromethane−ethyl acetate.

2: yield 58%; mp 222−223 °C (uncorrected); IR (CH_2Cl_2, 1.0 × 10^{-2} M) 3302 (N−H), 1742 (C═O), 1635 (C═O) cm^{-1}; ^{1}H NMR (400 MHz, $CDCl_3$) δ 8.96 (d, J = 7.4 Hz, 2H), 4.94−4.93 (m, 2H), 4.88−4.87 (m, 2H), 4.84 (quint, J = 7.4 Hz, 2H), 4.63 (dd, J = 4.2, 8.8 Hz, 2H), 4.52−4.50 (m, 2H), 4.29−4.27 (m, 2H), 4.18−4.06 (m, 4H), 3.94−3.88 (m, 2H), 3.72−3.67 (m, 2H), 2.35−2.26 (m, 2H), 2.14−2.07 (m, 4H), 2.05−1.97 (m, 2H), 1.37 (d, J = 7.4 Hz, 6H), 1.26 (t, J = 7.4 Hz, 6H); FAB-MS m/z 666 (M^+). Anal. Calcd for $C_{32}H_{42}N_4O_8Fe$: C, 57.66; H, 6.35; N, 8.41. Found: C, 57.53; H, 6.42; N, 8.32.

4: yield 61%; mp 171−172 °C (uncorrected); IR (CH_2Cl_2, 1.0 × 10^{-2} M) 3417 (N−H), 3317 (N−H), 1736 (C═O), 1682 (C═O), 1651 (C═O) cm^{-1}; ^{1}H NMR (400 MHz, $CDCl_3$) δ 8.58 (t, J = 6.0 Hz, 2H), 6.46 (d, J = 8.1 Hz, 2H), 4.86−4.84 (m, 4H), 4.66−4.60 (m, 2H), 4.44−4.38 (m, 4H), 4.21 (q, J = 7.2 Hz, 4H), 4.02 (dd, J = 6.4, 15.6 Hz, 2H), 3.86 (dd, J = 6.4, 15.6 Hz, 2H), 1.79−1.57 (m, 6H), 1.30 (t, J = 7.2 Hz, 6H), 0.98 (d, J = 6.0 Hz, 12H); FAB-MS m/z 670 (M^+). Anal. Calcd for $C_{32}H_{46}N_4O_8Fe$: C, 57.32; H, 6.91; N, 8.36. Found: C, 56.98; H, 6.89; N, 8.18.

5: yield 38%; mp 192−193 °C (uncorrected); IR (CH_2Cl_2, 1.0 × 10^{-2} M) 3410 (N−H), 3321 (N−H), 1736 (C═O), 1682 (C═O), 1651 (C═O) cm^{-1}; ^{1}H NMR (400 MHz, $CDCl_3$) δ 8.59 (t, J = 6.0 Hz, 2H), 7.34−7.19 (m, 10H), 6.47 (d, J = 7.6 Hz, 2H), 4.89−4.81 (m, 6H), 4.45−4.43 (m, 2H), 4.40−4.38 (m, 2H), 4.21−4.14 (m, 4H), 3.90 (dd, J = 6.4, 16.0 Hz, 2H), 3.81 (dd, J = 6.4, 16.0 Hz, 2H), 3.21−3.12 (m, 4H), 1.25 (t, J = 7.2 Hz, 6H); FAB-MS m/z 738 (M^+). Anal. Calcd for $C_{38}H_{42}N_4O_8Fe$: C, 61.79; H, 5.73; N, 7.59. Found: C, 61.39; H, 5.54; N, 7.59.

Synthesis of Ferrocene 3. To a stirred mixture of H-L-Ala-L-Pro-OEt·HCl (300.9 mg, 1.20 mmol) and triethylamine (836 μL, 6.0 mmol) in dichloromethane (5 mL) was added 1,1′-bis{(3-chlorocarbonyl)-propyl}ferrocene (236.3 mg, 0.60 mmol) in dichloromethane (10 mL) dropwise under argon at 0 °C. The mixture was stirred at 0 °C for 1 h and then at room temperature for 1 h. The resulting mixture was diluted with dichloromethane, washed with saturated $NaHCO_3$ aqueous solution and brine, and then dried over Na_2SO_4. The solvent was evaporated in vacuo, and the residue was chromatographed on an alumina column, eluting with dichloromethane to give **3**.

3: yield 48%; IR (CH_2Cl_2, 1.0 × 10^{-2} M) 3413 (N−H), 3321 (N−H), 1739 (C═O), 1643 (C═O) cm^{-1}; ^{1}H NMR (400 MHz, $CDCl_3$) δ 6.70 (d, J = 8.0 Hz, 2H), 4.79 (quint, J = 7.2 Hz, 2H), 4.49 (dd, J = 4.6, 8.2 Hz, 2H), 4.22−4.11 (m, 4H), 3.98 (br, 8H), 3.78−3.71 (m, 2H), 3.66−3.59 (m, 2H), 2.31−1.94 (m, 16H), 1.85−1.74 (m, 4H), 1.37 (d, J = 7.0 Hz, 6H), 1.26 (t, J = 7.2 Hz, 6H); FAB-MS m/z 750 (M^+). Anal. Calcd for $C_{38}H_{54}N_4O_8Fe·H_2O$: C, 59.37; H, 7.34; N, 7.29. Found: C, 59.29; H, 7.18; N, 7.11.

CD Measurements. CD spectra were recorded using a JASCO J-720 spectropolarimeter in the deaerated acetonitrile solution with the concentration (1.0 × 10^{-4} M) under an argon atmosphere at 25 °C.

Electrochemical Experiments. The cyclic voltammetry measurements were performed on a BAS CV-50W voltammetry analyzer in deaerated acetonitrile containing 0.1 M n-Bu_4NClO_4 as a supporting electrolyte at 25 °C with a three-electrode system consisting of a highly polished glassy carbon working electrode (BAS), a platinum auxiliary electrode (BAS), and an Ag/AgCl (0.01 M) reference electrode (BAS) at 100 mV/s scan rate. Potentials are given vs Fc/Fc^+ as an internal standard.

X-ray Structure Analysis. All measurements for **2** were made on a Rigaku AFC5R diffractometer with graphite-monochromated Mo Kα radiation and a rotating anode generator. All measurements for **5** were made on a Rigaku RAXIS−RAPID imaging plate diffractometer with graphite-monochromated Mo Kα radiation. The data of **4** were further refined.[9a] The structures of **2** and **5** were solved by direct methods and expanded using Fourier techniques. The non-hydrogen atoms were refined anisotropically. The H atoms involved in hydrogen bonding were located in electron density maps. The remainder of the H atoms were placed in idealized positions and allowed to ride with the C atoms to which each was bonded. Crystallographic details are given in Table 2.

Acknowledgment. This work was financially supported in part by a Grant-in-Aid for Scientific Research on Priority Areas from the Ministry of Education, Science, and Culture, Japan. Thanks are due to the Analytical Center, Faculty of Engineering, Osaka University, for the use of the NMR and MS instruments.

Supporting Information Available: Tables of X-ray crystallographics data for **2**, **4**, and **5** (PDF); X-ray crystallographic data (CIF). This material is available free of charge via the Internet at http://pubs.acs.org.

JA002869N